

Trends and perspectives of space-borne SAR remote sensing for archaeological landscape and cultural heritage applications

1 DEODATO TAPETE ^{a,*}, FRANCESCA CIGNA ^a

2

^a British Geological Survey, Natural Environment Research Council, Nicker Hill, Keyworth, NG12 5GG, UK;

* Corresponding author. Telephone: +44 (0) 115 936 3537

E-mail address: deodato@bgs.ac.uk

3

4 **ABSTRACT**

5 This paper provides an overview of the opportunities that image analysts, archaeologists and conservation
6 scientists currently have of using space-borne Synthetic Aperture Radar (SAR) imagery for prospection of
7 cultural landscapes and investigation of environmental, land surface and anthropogenic processes that can alter
8 the condition of heritage assets. The benefits of the recent developments in SAR satellite sensors towards higher
9 resolution (up to less than 1 metre) and shorter revisiting times (up to a few days) are discussed in relation to
10 established techniques using the two key SAR parameters – amplitude and phase. Selected case studies from
11 Middle East to South America illustrate how SAR can be effectively used to detect subtle archaeological
12 features in modern landscapes, monitor historic sites and assess damage in areas of conflict. These examples
13 form the basis to highlight the current trends in archaeological remote sensing based on space-borne SAR data
14 in the current era of the European Space Agency’s Sentinel-1 constellation and on-demand high resolution space
15 missions.

16 **KEYWORDS**

17 Radar remote sensing; SAR; amplitude; phase; change detection; archaeological remote sensing; damage
18 assessment; cultural heritage; Syria; Nazca

19 **1 INTRODUCTION**

20 This paper aims to provide an overview on the use of Synthetic Aperture Radar (SAR) images acquired from
21 space for purposes of archaeological landscape studies and cultural heritage applications, in recognition of the
22 increasing role that this branch of remote sensing is playing in the field of archaeological science.

23 Recent reviews have been published to illustrate the basic principles that make SAR suitable for archaeological
24 prospection (Lasaponara and Masini, 2013; Chen et al., 2015a) and showcase some successful achievements
25 with high resolution SAR sensors (Chen et al., 2015b). But an assessment of the current trends in SAR
26 archaeological remote sensing has not been carried out yet, alongside a review of the existing opportunities
27 offered by the recent technological developments.

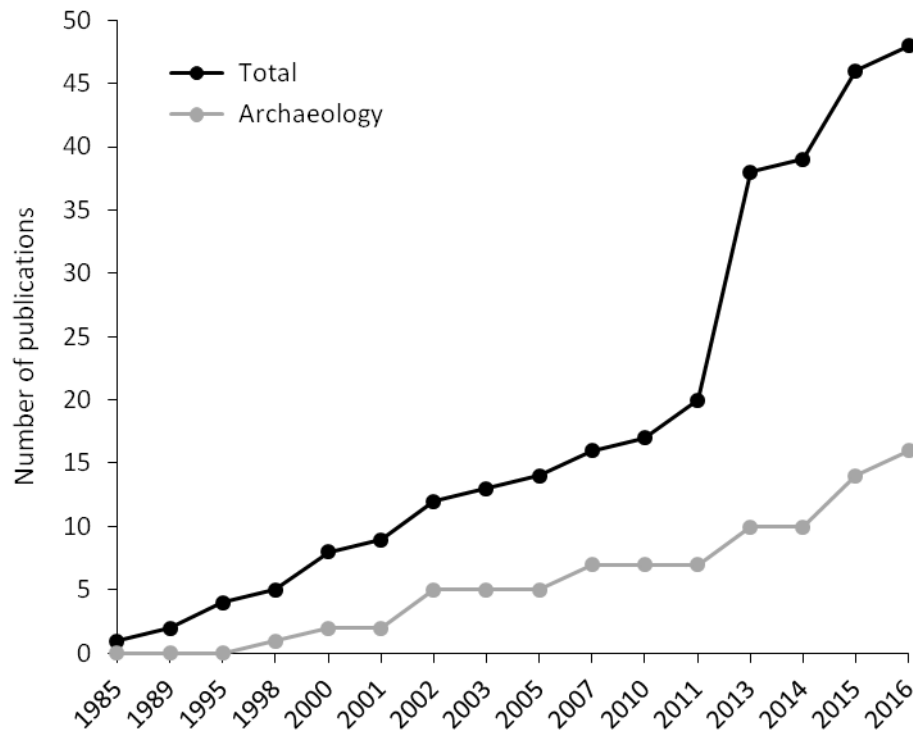
28 It is to fill this gap that in this paper we review the three key factors – data, processing methods and application
29 types – that at present favour the exploitation of this space technology to complement well-established
30 techniques of aerial photography, optical remote sensing and generation of digital elevation models (DEMs).

31 **2 BACKGROUND AND GROWING IMPACT**

32 From an historical perspective, the earliest use of SAR to study paleo-landscapes dates back to the 1980s with
33 investigations in both tropical and subtropical territories (Adams et al., 1981) and arid environments (Elachi et
34 al., 1984). Since then, several studies revealed hidden features and paleo-landscapes, by exploiting the peculiar
35 penetration capability of the radar signal (El-Baz, 1998; Lira et al., 2005; Wiseman and El-Baz, 2007; Evans et
36 al., 2007; Moore et al., 2007) at the different microwave bands of acquisition, i.e. *L* 1-2 GHz, 15-30 cm; *C* 4-8
37 GHz, 3.75-7.5 cm; *X* 8-12.5 GHz, 2.5-3.75 cm, and proving that better performance is usually obtained at longer
38 wavelengths (*L*- > *X*-band) and in drier and fine-grained soils.

39 A proof of evidence of the growing scientific relevance that SAR is assuming in this field is gathered in Figure
40 1. Using a similar approach to that described by Agapiou and Lisandrou (2015), a Scopus engine search of the
41 keywords 'radar', 'remote sensing', 'archaeology', 'cultural heritage' and 'polarimetry', highlights that there has
42 been a significant increase of indexed peer-reviewed publications focussed on the use of SAR for archaeological
43 science in the last 30 years (series “Total” in Figure 1). A steady increase is observed until 2011, while the
44 publication boost occurred in 2013 with the publication of a dedicated special issue on *Archaeological*
45 *Prospection*. Although this search is not exhaustive (and does not pretend to be so), it provides an interesting

46 and objective bibliometric. The analysis of authors' affiliations also reveals that one third of the total number of
47 these publications has involved research teams including archaeologists (series "Archaeology" in Figure 1), and
48 confirms that teamwork between archaeologists and remote sensing experts is increasing since the late 1990s.
49



50

51 **Figure 1:** Graph of publications (series "Total") since 1985 that are indexed in Scopus and specifically use SAR
52 for studies of archaeological landscapes, archaeological prospection and condition assessment of cultural
53 heritage. The series "Archaeology" refers to those publications among the "Total" that are co-authored by
54 archaeologists.

55

56 Matching evidence is found in Agapiou and Lisandrou (2015) who report that 'radar images' are among the most
57 frequently used terms in the relevant remote sensing literature between 2013 and 2015.

58 The large percentage of the published research is based on the use of the 'amplitude', i.e. the magnitude of the
59 microwave wavelength recorded for each pixel of the complex SAR image. The 'radar backscatter' as the portion
60 of the outgoing radar signal recorded over successive pulses from elements of a synthetic aperture to create the
61 image, is mostly analysed to infer the compositional and soil moisture properties of the radar targets on the
62 ground and associate them to surface changes that may relate to buried features.

63 The other main group of publication concentrates on the use of DEMs generated with Interferometric SAR
64 (InSAR) techniques, by which the measured differences in the phase of the return signal between two satellite

65 passes is used to combine two radar acquisitions of the same area of the Earth's surface, taken from slightly
66 different angles, to generate accurate height maps (ESA, 2015).

67 **3 CURRENT OPPORTUNITIES FROM SPACE**

68 The scientific advancement of satellite radar research for archaeological studies was possible owing to an
69 increasing availability, from the early 1990s, of SAR imagery in the catalogues of the space agencies, covering
70 with more regular frequency not only the Western countries but also remote areas of South America, Asia and
71 Africa. Furthermore, since the early 2000s, the beam modes with which SAR images are acquired have been
72 continuously improved, so that nowadays image analysts, archaeologists and conservation scientists can access
73 data with: wide-swath to spotlight coverage, kilometre to sub-metre spatial resolution, historical and present
74 dates of acquisition, longer to shorter wavelength (L/C/X bands), monthly to daily revisiting time if collecting
75 time series.

76 At present radar remote sensing is witnessing the revolutionary turn of the satellites from the first (e.g., ERS-
77 1/2, ENVISAT, ALOS, RADARSAT-1/2) to the second generations (e.g., TerraSAR-X, COSMO-SkyMed,
78 Sentinel-1 and ALOS-2). In this context there is a range of opportunities for feature detection, condition and
79 damage assessment (Tapete et al., 2015c, 2016).

80 **3.1 Space-borne data**

81 **3.1.1 Legacy SAR archives**

82 The ERS-1/2 and ENVISAT catalogues of the European Space Agency (ESA) are the most complete and
83 abundant archives of C-band time series, with almost uninterrupted temporal coverage from 1991 to April 2012.
84 Their Image Mode spatial resolution of 25-30 m and swaths of 100 km make these images suitable for wide-
85 area and regional assessments (e.g. detection of paleo-channels, trade route reconstruction), alongside
86 investigation of sites as wholes and contextualised in their surrounding environments (Figure 2a).

87 Similarly, the archives built by the Japanese Space Agency (JAXA) with the L-band ALOS PALSAR sensor
88 provide an historical view of cultural landscapes from 2006 to May 2011, with resolution up to 7 m in Fine
89 Beam mode, both single and dual polarised (HH, VV, HH+HV, VV+VH). Kurtcebe et al. (2010) and Guo et al.
90 (2011) are among the earliest studies showcasing the usefulness of ALOS PALSAR in archaeology, while more

91 research may be carried out to fully exploit the archives available over those regions in India, South America
92 and Pacific Ocean where ancient civilizations settled and flourished for centuries.

93

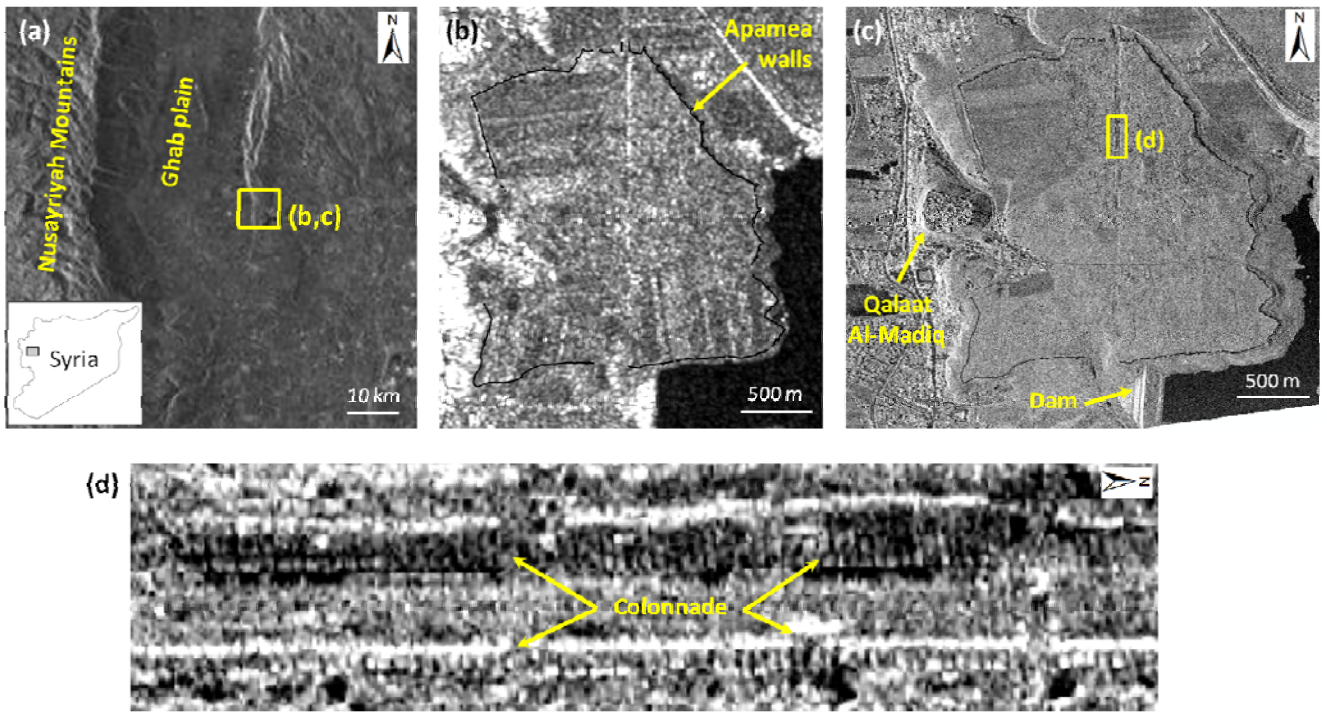
94 **3.1.2 New satellites and SAR imaging modes**

95 The TerraSAR-X constellation of the German Aerospace Center (DLR) is a clear example of how on-demand
96 high to very high resolution SAR can nowadays support studies of archaeological landscapes and sites by
97 providing a range of different resolutions, up to unprecedented sub-metre level imaging.

98 Acquiring X-band imagery since mid-2007 with the twin satellite TanDEM-X launched three years later,
99 TerraSAR-X (TSX) is building an image archive with repeat cycle of 11 days (i.e. a third of ESA's first
100 generation sensors) and a range of spatial resolutions, from 16 m and scene size of 100 km (width) x 150 km in
101 ScanSAR mode, to azimuth resolution of 0.24 m over scene extent varying between 2.5 to 2.8 km in azimuth
102 and 4.6 to 7.5 km in range in Staring Spotlight mode (Mittermayer et al., 2014).

103 The Hellenistic town of Apamea, Syria, well demonstrates the paradigm of multi-temporal and multi-scale
104 analysis using different satellites. ScanSAR time series 2011-2014 (Figure 2b) complemented the historical
105 analysis with ERS-1/2 and ENVISAT by providing a regional scale coverage to assess the recent impact on
106 landscape due to the construction of the dam nearby the Justinian walls (see section 3.2.4) and the agricultural
107 activities in the Ghab plain (Figure 2a). Coeval sub-meter resolution Staring Spotlight imagery (Figure 2c;
108 Tapete et al. 2016), instead, allows up-scaling of the observations at the level of individual structures, such as
109 the monumental colonnade of Apamea (Figure 2d). Given the current exposure of the site to war damages,
110 looting and vandalism, the strong backscatter return from the marble columns provides a reliable SAR marker to
111 assess whether the ancient ruins are still standing or collapsed (see section 4.2).

112



113

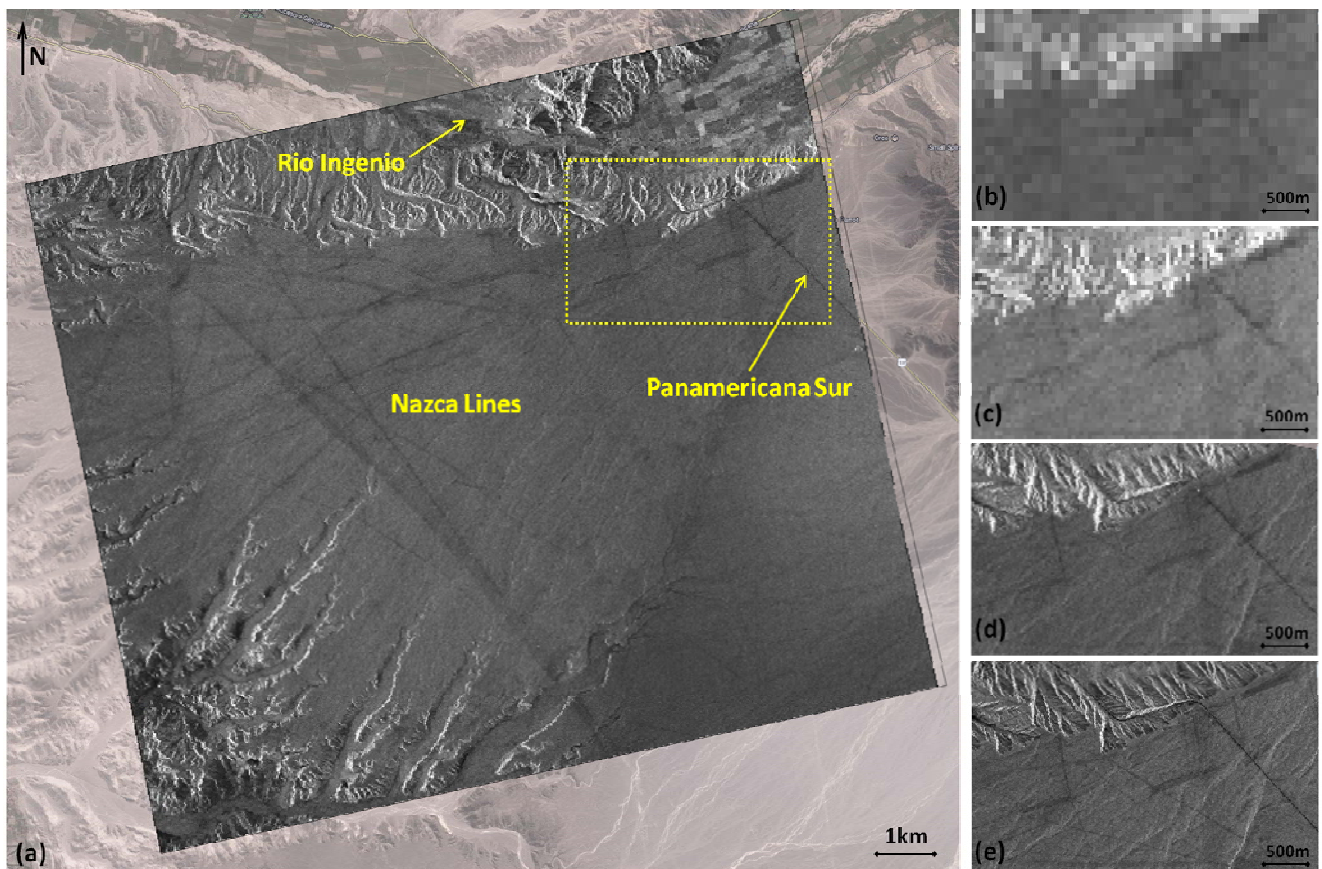
114 **Figure 2:** SAR opportunities for site investigation. (a) 25-m resolution ENVISAT IS2 VV, 9 June 2006, (b) 17-
 115 m geocoded TerraSAR-X ScanSAR, 17 May 2011 (© DLR 2016), and (c) 0.24-m resolution geocoded Staring
 116 Spotlight ascending mode image, 27 December 2014 (© DLR 2016) of Apamea, western Syria. (d) Detail of the
 117 monumental colonnade from the Staring Spotlight mode, enhancing the unprecedented very high spatial
 118 resolution currently achievable with space-borne SAR.

119

120 Archaeologists can also benefit from the full range of beam modes and incidence angles offered by the same
 121 satellite mission to improve the detection and delineation of subtle archaeological features, whilst relating them
 122 to the landscape over a wide swath. Figure 3 demonstrates the stunning improvement in SAR imaging from
 123 ScanSAR to High Resolution Spotlight modes to discriminate the UNESCO World Heritage List Nasca Lines,
 124 in Southern Peru. The distinctive radar signature of the 'negative geoglyphs' (exposed unpatinated and lighter
 125 coloured ground) can be analysed by drawing a backscatter profile from the feature to the nearby soil (dark
 126 gravels) and checking its consistency or variations by year or by season (Tapete et al., 2013b).

127

128



129 **Figure 3:** SAR opportunities for feature detection. (a) TerraSAR-X (TSX) SpotLight 13 August 2008 ascending
130 mode with VV polarization, 32.5°-33.6° incidence angles over the Nasca Lines (© DLR 2016), overlapped onto
131 optical imagery (© 2013 Google Imagery © Cnes/Spot Image, DigitalGlobe, Map data © Google). Comparison
132 of: (b) ScanSAR TSX, HH, ascending, range res. 17.0-19.2 m; (c) StripMap TanDEM-X (TDX), HH,
133 ascending, range res. 3.3-3.5 m; (d) SpotLight TSX, HH, descending, range res. 1.7-3.5 m; (e) High Resolution
134 SpotLight TDX, HH, descending, range res. 1.1-3.5 m (© DLR 2016) (modified from Tapete et al., 2015b).

135

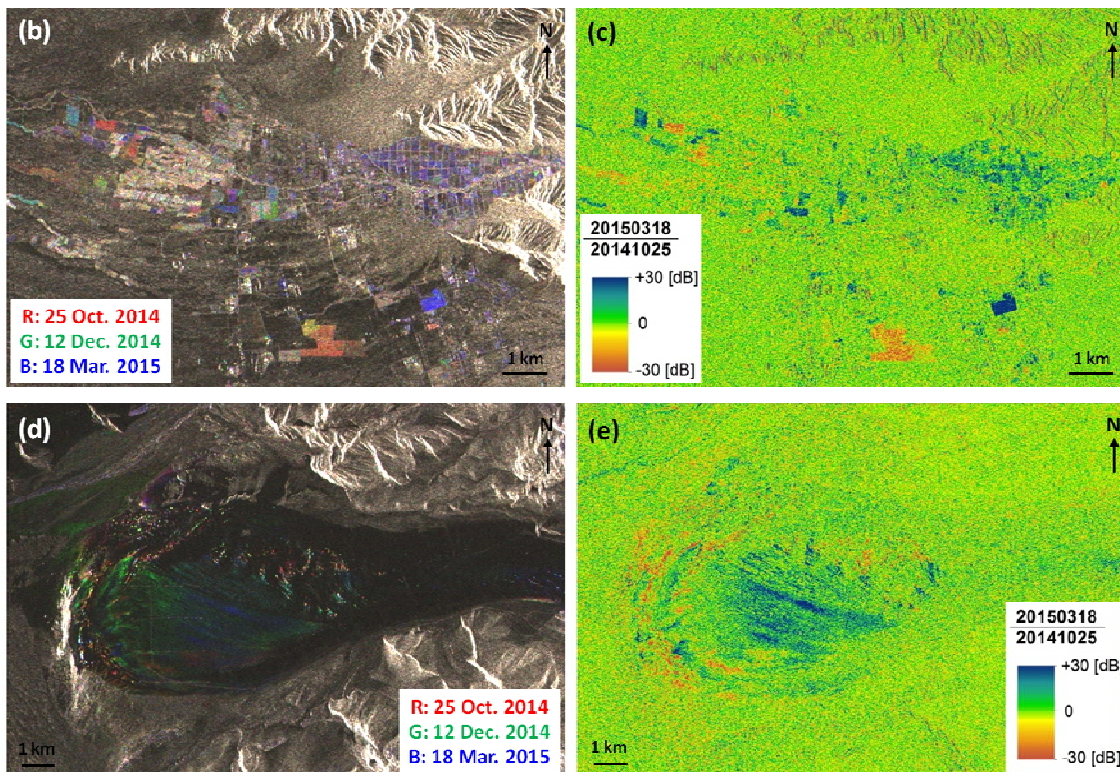
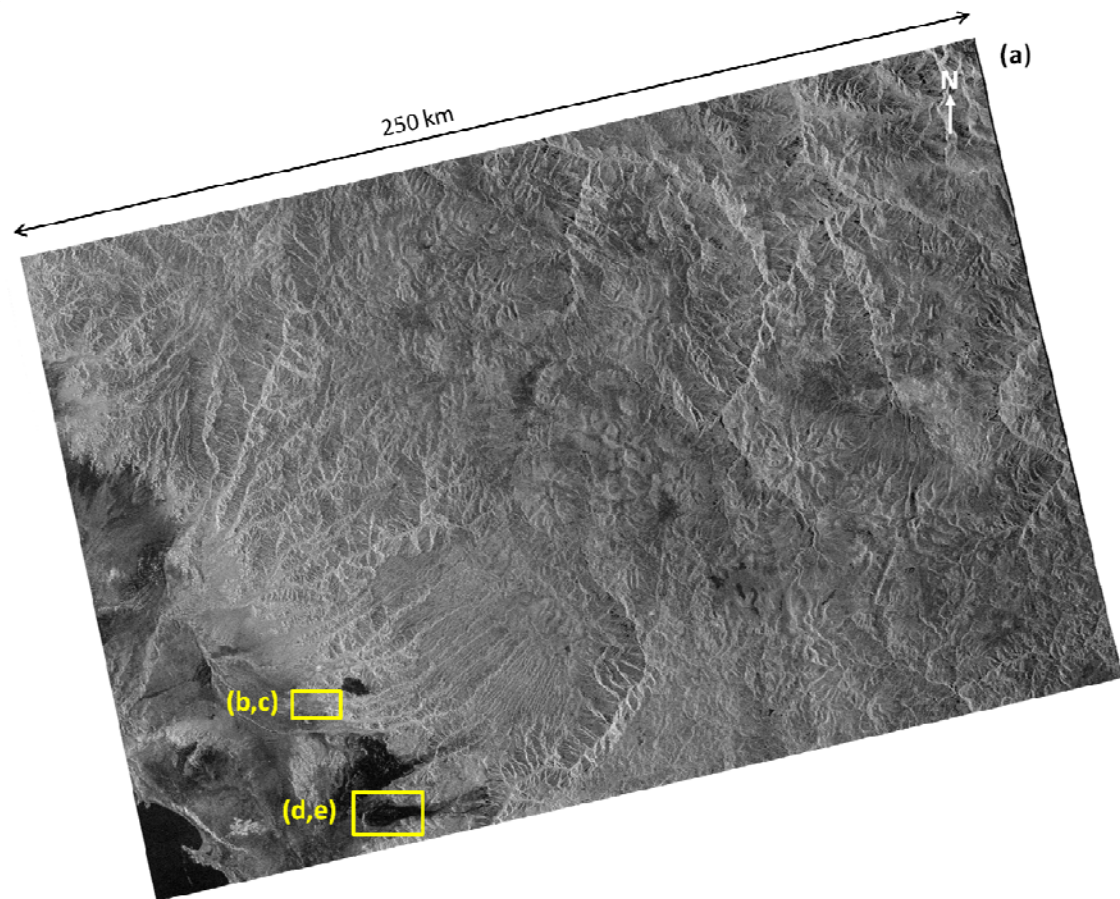
136 The suitability of SAR remote sensing to the specific purpose of investigating archaeological landscapes relies
137 on the flexibility offered by the radar sensors to tune up the acquisition parameters. In this regard the successor
138 to ALOS PALSAR – namely ALOS-2, launched in May 2014 – can acquire images with single to full
139 polarization, range-azimuth resolution up to 3 x 1 m and incidence angles between 8 to 70 degrees in the various
140 beam modes. Operating in L-band, the sensor PALSAR-2 is expected to penetrate more of the topsoil,
141 depending on the incidence angle (see section 3.2.3) at equal environmental conditions (e.g., feature roughness
142 and soil moisture).

143 Conversely, the coeval ESA C-band Sentinel-1A satellite launched in April 2014, with its twin Sentinel-1B
144 launched in April 2016, is building a consistent and regular SAR catalogue with the pre-defined Interferometric
145 Wide swath (IW) mode acquiring data at 5 m by 20 m spatial resolution over 250 km swaths (see the example in

146 Figure 4a in southern Peru), allowing conflict-free high resolution coverage of dual polarisation and
147 interferometric data potentially over all global landmasses (ESA, 2013). The RGB and amplitude change
148 detection analyses presented in Figure 4b-d are exemplars of how the use of regular Sentinel-1 acquisitions
149 allows surface properties (e.g. soil moisture, location and displacement of landforms) to be monitored, and used
150 as a proxy to infer changes due to human activities or natural processes in the landscape. Under a conservation
151 perspective, this is the area where the Sentinel-1 constellation can be valuable for purposes of routine
152 monitoring and condition assessment over wide areas. Emergency observation requests altering the pre-defined
153 Sentinel-1 observation scenario are foreseen, possibly exploiting the 5 x 5 m resolution StripMap (SM) mode
154 over narrow swath width of 80 km with adjustable beam incidence angle and the elevation beamwidth (ESA,
155 2013). Section 4.3 illustrates a simulation of the operational capability of Sentinel-1 SM in such a circumstance
156 (Tapete et al., 2015c).

157 A further element that, undoubtedly, will encourage the use of Sentinel-1 data is their accessibility. The data are
158 free for download and use from the Sentinels Scientific Data Hub (<https://scihub.esa.int/>), in various formats,
159 i.e. SAR Level-0 (compressed and unfocused SAR raw data), Level-1 (focused data) and Level-2 (geo-located
160 geophysical products). In particular, Level-1 Ground Range Detected (GRD) products are focused SAR data
161 that have been detected, multi-looked and projected to ground range using an Earth ellipsoid model, and
162 provided in GeoTIFF format. These raster images have approximately square resolution pixels and square pixel
163 spacing with reduced speckle, although at the cost of reduced geometric resolution and loss of phase
164 information. Although this means that interferometric analysis is not possible with GRD products, image
165 analysts can use them straightforward with GIS software for purposes of amplitude change detection (see
166 section 3.2.1) or geospatial analysis and data integration.

167 An example of the readiness of these data for use is provided in Figure 4. Sentinel-1A data over the area of the
168 Nasca Civilisation in southern Peru were downloaded from the Sentinels Scientific Data Hub and processed
169 using basic GIS geoprocessing tools to normalise the radar reflectivity of the image pixel as per the Sentinel-1
170 User Handbook (ESA, 2013) and generate the RGB color composite and the amplitude ratio using the formula
171 reported in section 3.2.1.



172

173 **Figure 4:** (a) Sentinel-1 IW image of the Rio Grande drainage basin in Peru acquired on 25 October 2014 with
 174 VV polarisation. (b,d) RGB colour composites and (c,e) image ratios for the area of (b-c) Rio Taruga where soil
 175 moisture changes can be recognised in the agricultural fields along the river plain and (d-e) a sand dune where
 176 wind-driven mass movements occur.

177

178 Nonetheless, whilst the accessibility to Sentinel-1 images has to be recognised as an opportunity for the
179 archaeological community, it is still to determine whether archaeologists already embrace the usefulness of
180 these data, see value for their research purposes and have the necessary skills to use them without the support of
181 image processing analysts. Training and skill development should be part of the process to transfer this
182 technology into the archaeological science practice. In this regard, education initiatives promoted by the image
183 providers are welcome. A recent example is the 3rd course on remote sensing for archaeology organised by ESA
184 and the European Association of Remote Sensing Laboratories - EARSel (ESA-EARSel, 2015), with specialist
185 training sessions on the use of SAR data for change detection (Tapete & Cigna, 2015).

186

187 **3.2 Processing methods**

188 SAR processing methods can be distinguished by the radar parameter used: amplitude and radar backscatter;
189 coherence; polarisation; phase.

190

191 **3.2.1 Amplitude change detection**

192 This method allows the investigation of spatial and temporal changes of the backscattering coefficient σ^0 that
193 indicates the radar signal backscattered to the sensor, normalized – to a first approximation – to the horizontal
194 ground surface and referred to as per unit area on the ground.

195 Cigna et al. (2013) illustrate the typical workflow to extract, convert to decibel (dB) and analyse values of σ^0 for
196 purposes of change detection. An example of amplitude change detection consists in the computation of ratios
197 between SAR pairs. Two SAR images k and j acquired by using the same acquisition mode and geometry at the
198 times t_k and t_j respectively are spatially filtered to reduce the effects of radar speckle and increase the signal
199 content of the image pixels. Their backscatter ratio (R_{σ^0}) is computed, pixel by pixel, as follows:

$$R_{\sigma^0} = \frac{\sigma_i^0(t_k)}{\sigma_i^0(t_j)}$$

200

201 where R is a dimensionless parameter which takes on values between 0 and 1 when the considered pixel i has
202 higher backscattering coefficient at the time j with respect to time k , while values exceeding 1 occur when the
203 pixel i has lower backscattering coefficient at the time j with respect to time k .

204 The result is a map showing the spatial patterns of σ^0 increase and decrease (Figure 5a-b) that offers potential
205 for correlation with changes in soil moisture content, vegetation coverage or morphology, the latter being for
206 instance due to legal or illegal excavations, collapses or demolitions (see section 4.3).

207

208 **3.2.2 Multi-temporal coherence**

209 Coherence (γ) is a measure of interferometric phase correlation, and can be computed as the cross-correlation
210 coefficient of two SAR images that is estimated over a small window of a few pixels in range and azimuth, once
211 all the deterministic phase components (mainly due to the terrain elevation) are compensated for (ESA, 2007).

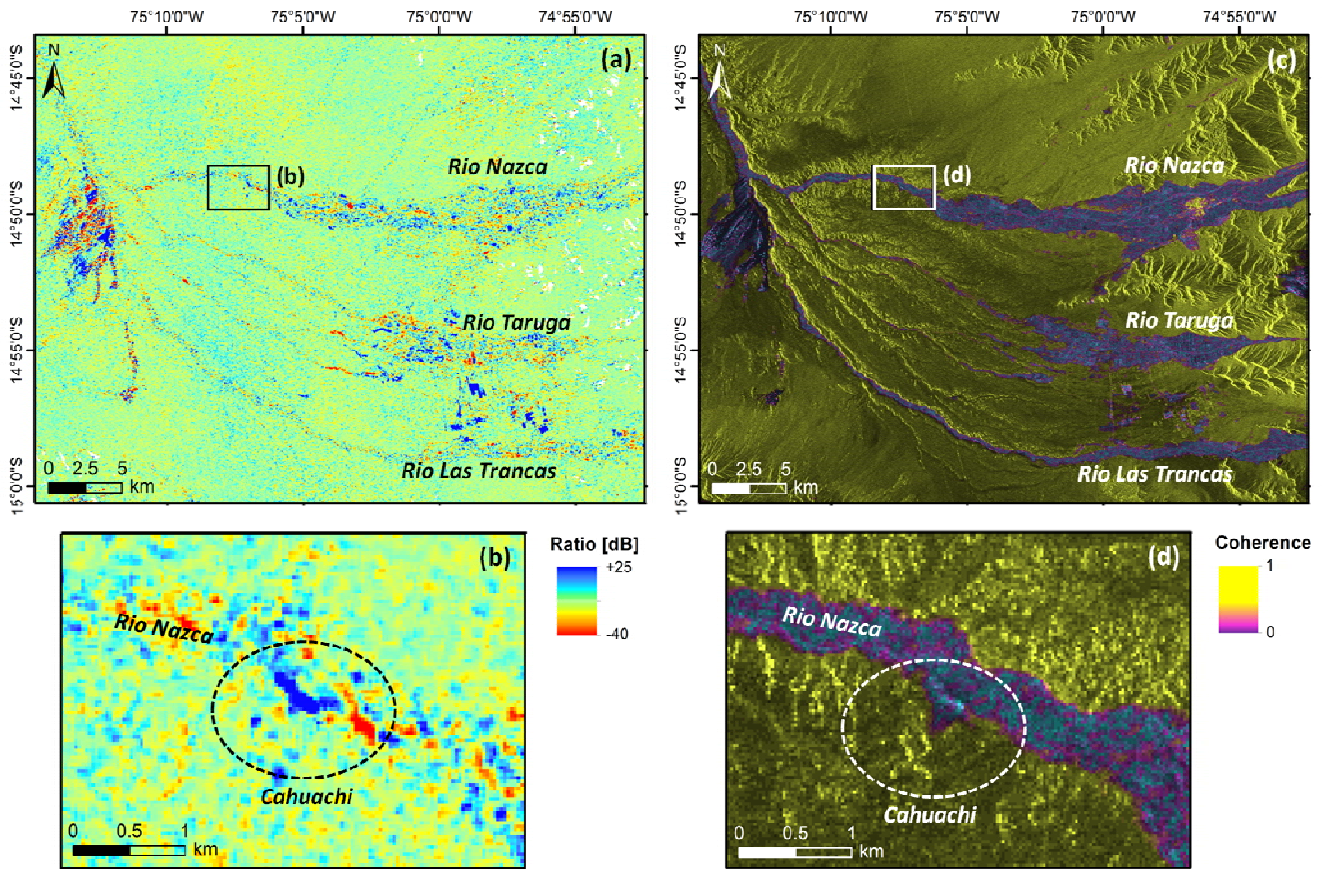
212 Computation of the absolute value of γ using a moving window over the whole SAR image results in a
213 coherence map of the observed scene, where values can range from 0 to 1, i.e. from no to perfect correlation.

214 Strong coherence means high homogeneity with no change of land surface properties such as soil moisture,
215 vegetation cover, roughness, elevation or geometry, whilst low γ values are found over altered surfaces.

216 Figure 5 shows how coherence maps can complement an amplitude-based change detection analysis, while
217 Figure 6 demonstrates the benefit of multi-temporal coherence maps to track changes in the landscape induced
218 by anthropogenic activities (e.g. archaeological excavations) and land surface processes and properties (i.e. soil
219 moisture).

220 Between 2005 and 2007 R_{σ^0} patterns were observed in association with loss of coherence in the floodplain of
221 Rio Nazca, Peru, in proximity to Cahuachi, the world largest adobe ceremonial centre (Tapete et al., 2013b).
222 Historically the whole area was affected by flood events to the extent that the settlements were heavily damaged
223 or destroyed (Cigna et al., 2013). Although the river brings fresh mud yearly, thereby creating a fertile strip for
224 agriculture, it still represents a treat for the local archaeological heritage, also due to extreme meteorological
225 events occurring in the mountain range to the east of the plain. Alteration of the radar backscatter between dry,
226 wet and flooded un-vegetated surfaces can be also used to infer the impact in the recent past and assess flood
227 hazard and susceptibility.

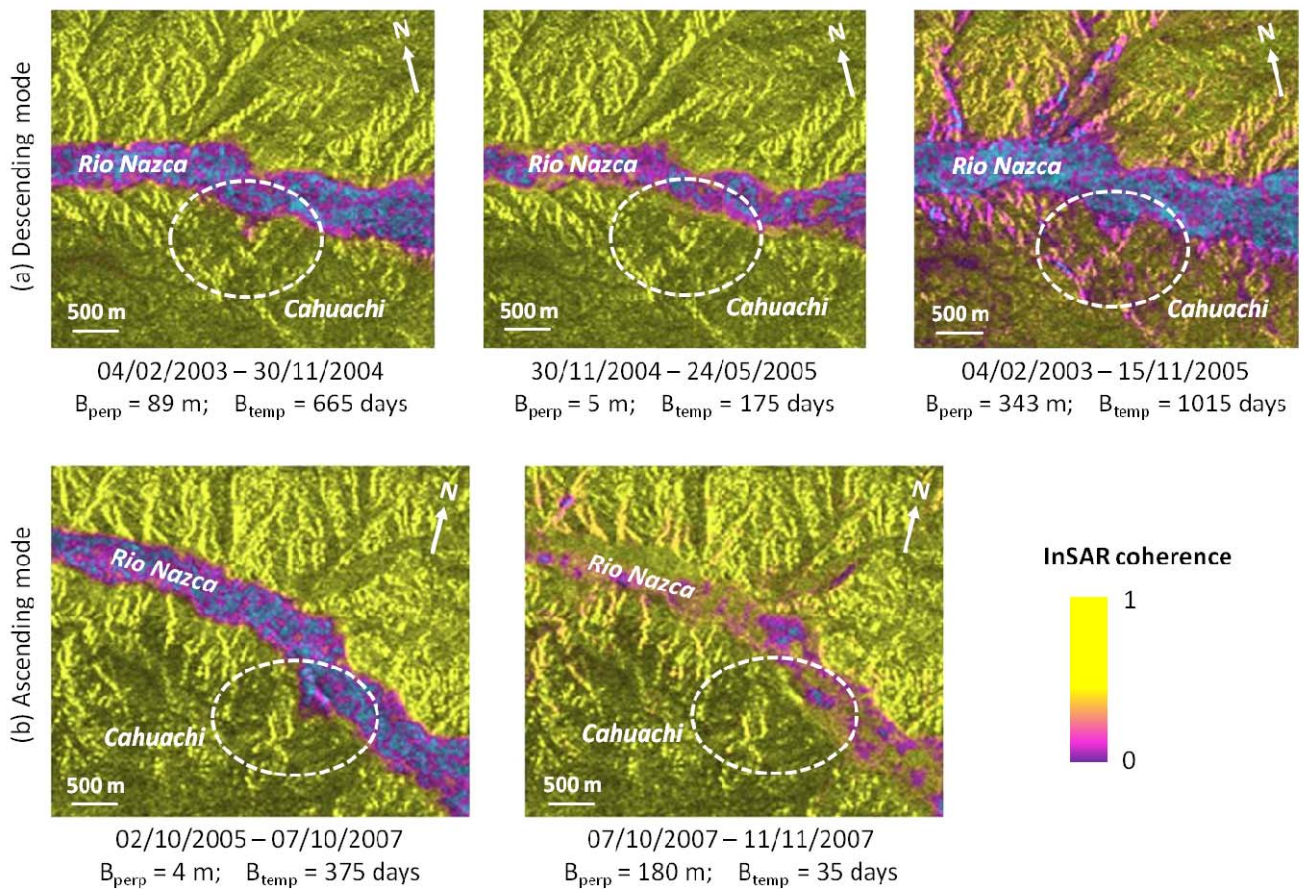
228



229

230 **Figure 5:** Change detection maps based on (a-b) the ratio of the backscattering coefficient between ENVISAT
 231 ascending mode images acquired on 2 February 2005 and 7 October 2007, and (c-d) the corresponding
 232 coherence maps (perpendicular baseline 4 m) over the Nasca Civilisation region in Peru and the archaeological
 233 site of Cahuachi. The dotted circles highlight areas where changes in the ratio (blue-red patterns) are associated
 234 with loss of coherence (pink-purple patterns) likely due to soil moisture and vegetation changes along the river
 235 plain as seen in (a) for the Rio Nazca, Taruga and Las Trancas plains, and archaeological excavations in the area
 236 of the ceremonial centre of Cahuachi.

237



238

239 **Figure 6:** InSAR coherence maps for (a) descending and (b) ascending mode ENVISAT ASAR pairs for the
 240 area of Cahuachi in Peru in the period 2003-2007, highlighting decorrelation due to soil moisture changes along
 241 the Rio Nazca flood plain, and backscattering variations in the areas of archaeological excavations in the
 242 ceremonial centre of Cahuachi. B_{temp} = temporal baseline; B_{perp} = perpendicular baseline.

243

244 3.2.3 Polarimetric SAR (PolSAR)

245 Polarimetry is the measurement and interpretation of the polarization of electromagnetic waves and, for
 246 archaeological prospection, is used to detect proxies indicating the existence of buried features. SAR scattering
 247 mechanisms of the targets on the ground may differ as a consequence of the type and health of overlying
 248 vegetation (Stewart et al., 2014).

249 The typical PolSAR workflow consists of: multi-looking to reduce speckle and obtain a squared pixel (or multi-
 250 temporal averaging in the case of a stack of SAR images); analysis of target decompositions; extraction and
 251 analysis the polarimetric signatures to enhance the visibility of suspected buried structures. As demonstrated by
 252 Dore et al. (2013) in the sites of Samarra, Iraq, and Djebel Barkal, Sudan, Pauli RGB image of multi-looked
 253 polarimetric SAR data is the first qualitative map to identify areas of different polarimetric response, while

254 polarimetric descriptors of entropy (H) and alpha angle (α) are obtained by extracting the coherency matrix T3,
255 to quantitatively analyse the randomness of the scattering mechanism and assess the predominant scattering
256 mechanism between single-bounce, double-bounce or volume scattering. The contribution of these three
257 mechanisms can be then modelled using the Freeman decomposition (Dore et al., 2013), especially when
258 ground-truth measurements are not available.

259 Patruno et al. (2013) provide an interesting discussion about how different bands, incidence angles and spatial
260 resolution can be negotiated in a polarimetric analysis to detect subtle to buried features. In the case of Samarra,
261 although L-band ALOS PALSAR imagery is expected to penetrate more of the topsoil, better results are
262 obtained with the higher resolution C-band RADARSAT-2 full-polarization image acquired with 26.63°
263 incidence angle to detect the *qanāt* outside the octagonal city. This configuration also proves more suitable than
264 the RADARSAT-2 image at 43.43° incidence angle.

265 Fully polarimetric ALOS PALSAR and RADARSAT-2 images have been also recently used by Gaber et al.
266 (2013, 2015) to detect and characterize a well-defined geometric target hidden under sand deposits in the
267 Western Desert of Egypt and classify the surface sediments along El-Gallaba Plain.

268 These examples further confirm that PolSAR can be very helpful in dry and arid environments, where no
269 interference is caused by soil moisture. Nevertheless, research is needed to assess at what extent PolSAR can
270 support archaeological studies also in temperate zones and exploit the highest resolution SAR beam modes and
271 the flexibility of incidence angle offered by the current space missions.

272

273 **3.2.4 DEM generation**

274 To generate DEMs from radar data, SAR image pairs are acquired by two sensors flying along parallel tracks in
275 across-track formation (not dissimilar to stereo-composition of optical sensors), so as the same point on the
276 ground is imaged simultaneously from two slightly different directions. The typical workflow to generate DEMs
277 with Interferometric SAR processing (InSAR) is fully discussed in ESA (2007).

278 InSAR DEMs of Earth's surface have been generated since the 1990s, during the Space Shuttle SIR-C/X-SAR
279 missions in 1994 and the 'tandem' mission of ESA's ERS-1 and ERS-2 satellites from 16 August 1995 until
280 mid-May 1996, with ERS-1 and ERS-2 phasing of 1 day (ESA, 2007). In February 2000 the first single-pass
281 radar interferometer in space flew onboard NASA's Shuttle Radar Topography Mission (SRTM; Farr et al.,
282 2007), which generated the first homogeneous, validated and freely available 90 m resolution global Digital

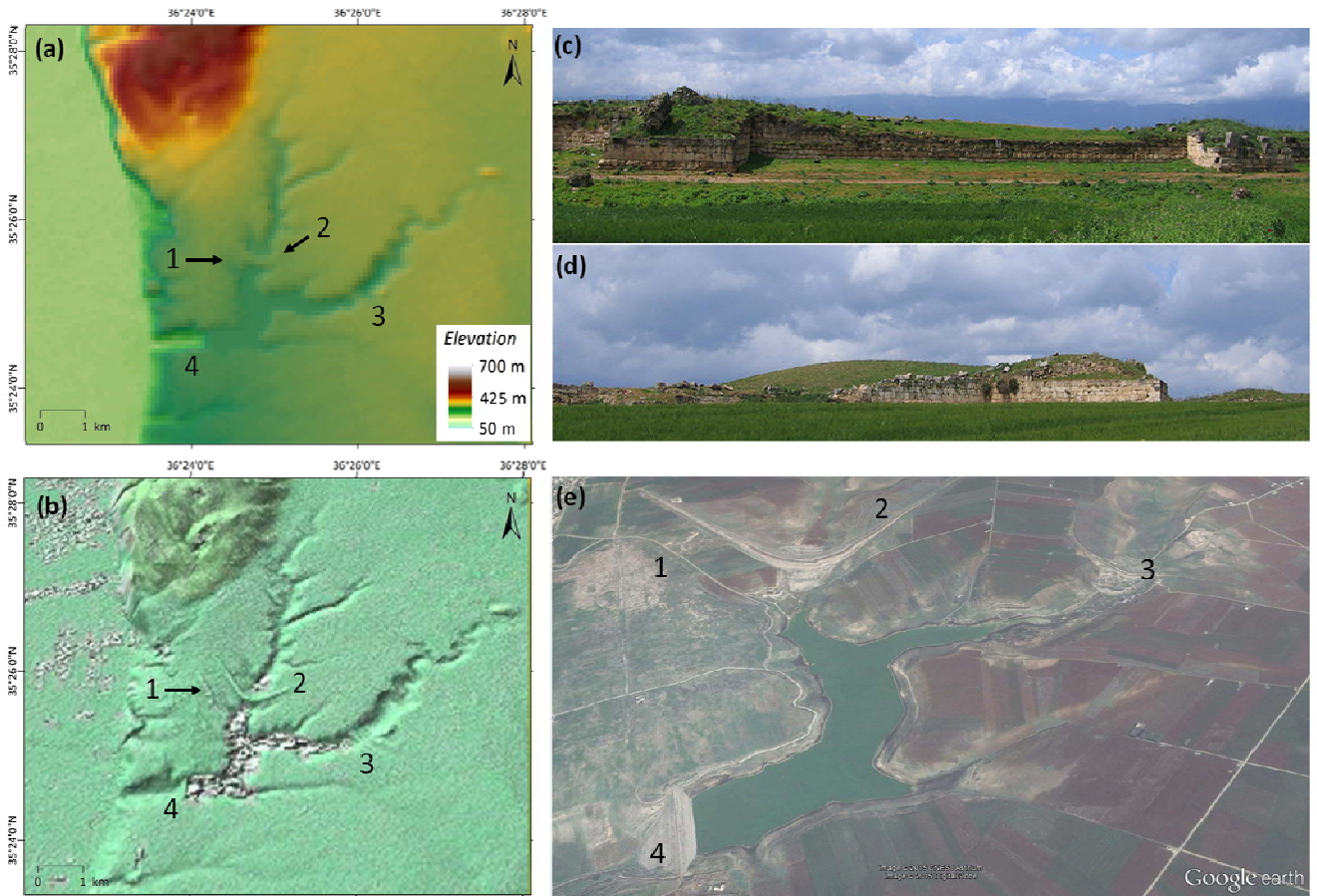
283 Surface Model (DSM) of the Earth. Figure 7a shows the SRTM DSM over the archaeological site of Apamea,
284 Syria, from which the main topographic features and the northern dam are clearly visible.

285 Papers published in Wiseman and El-Baz (2007) report various examples where SRTM was used to extract
286 slope and elevation information in combination with land cover maps and natural resource mapping, to identify
287 anthropogenic settlements, trade routes and migration pathways, alongside prediction of future flood and
288 landslide hazards.

289 The release, since 2014, of the global 1 arc-second (~30 m) resolution SRTM elevation data will certainly push
290 the landscape research forward, owing to the improved resolution compared to the 90 m of the previous product
291 that, in recent years, scholars already proved to be valuable for archaeological prospection (e.g. Blom et al.,
292 2000 for tracking trade routes; Menze et al., 2007 for mapping ancient settlement mounds).

293 In this context, DLR's TanDEM-X mission is revolutionary. In addition to the generation of a worldwide,
294 consistent and high precision global DEM at 12 m resolution, StripMap (SM) and High Resolution Spotlight
295 (HS) data at 3 and 2 m resolution are acquired using the operational alternating bistatic and monostatic
296 acquisition modes. A comprehensive quantitative appraisal of the absolute and relative vertical accuracy of
297 these elevation products in an archaeological context was recently published by Erasmi et al. (2014). The
298 authors showed that SM data were suitable to reconstruct a paleo-channel in the alluvial plain of Cilicia, Turkey,
299 and enhanced the micro-topography of fortification towers, gates, theatre and stadium of the ancient city of
300 Magarsos using HS data.

301



302

303 **Figure 7:** (a) 90 m resolution SRTM DSM, (b) shaded relief of 3-m resolution TanDEM-X StripMap Bistatic
 304 HH DEM 27 February 2012 (© DLR 2016) with indication of the archaeological and landscape features of
 305 interest for the site of Apamea, Syria (see Figure 2): 1) eastern Justinian walls; 2-4) dams of the Apamea lakes.
 306 (c-d) Details of the eastern walls prior to looting; (e) Google Earth image of the Apamea lake and dams (© 2015
 307 CNES/Astrium; © 2015 DigitalGlobe).

308

309 Similar results are obtained in Apamea (Figure 7). SM bistatic DEM HH polarization not only improves the
 310 delineation of the three dams of the Apamea lake and the topographic features of the natural relief where the
 311 ancient town was built, but also allows the recognition of the eastern walls (Figure 7b-d). This is a clear
 312 example of the usefulness of these data to analyse the regional context in which a site can be studied up to the
 313 local scale, and anthropogenic impacts on the landscape can be assessed.

314 Access to high resolution DEMs based on satellite SAR data is an opportunity for archaeological research in
 315 those areas across the world where the feasibility of LiDAR data collection from airborne platforms is limited
 316 not only due to environmental (cloud-coverage) or funding issues, but also security considerations, such as in
 317 sensitive areas or un-accessible regions.

318 4 CULTURAL HERITAGE AND LANDSCAPE APPLICATIONS

319 4.1 *Detection of archaeological features*

320 Given the legacy of historical data and the diverse options for new acquisition with the current space missions
321 (see section 3.1), it would be simplistic and reductive to state that only highest resolution SAR imagery should
322 be used for detection of archaeological features. Images are to be selected accounting for the size, morphology,
323 location and degree of exposure of the features on the ground to investigate.

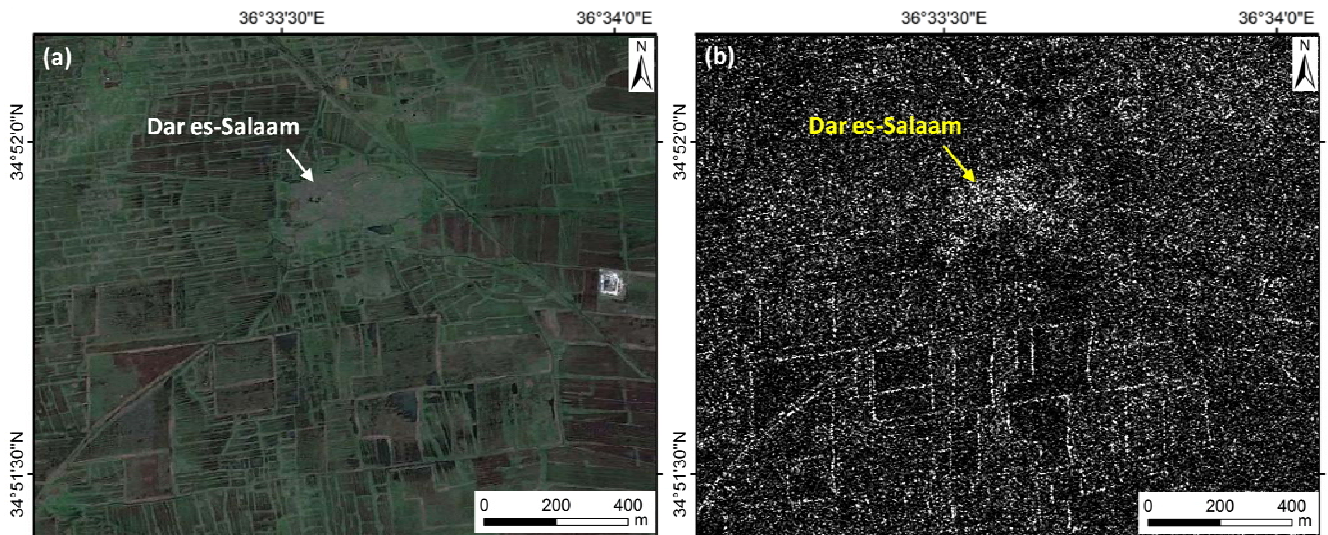
324 Tapete et al. (2013b) demonstrated that even medium resolution SAR images such as 30 m resolution
325 ENVISAT ASAR were suitable to delineate major geoglyphs of Nasca Lines or detect buried and abandoned
326 *puquios*, although the obvious limitation relates to the precision with which the feature is delimited from the
327 nearby soil and its land use. Furthermore, despite their lower resolution, historical data are sometimes the only
328 imagery available from the space agencies' archives, and can be used to look at past landscapes that have been
329 modified by human actions such as extensive ploughing, dam construction, urban sealing, war damages and
330 vandalism.

331 At present, except for the L-band ALOS-2 mission, the highest resolution SAR imagery is acquired in X-
332 band (e.g., TerraSAR-X Staring Spotlight and COSMO-SkyMed Spotlight; Figure 2d) which is expected to
333 have lower penetration capability than L-band, at equal environmental conditions. As mentioned in section
334 3.2.3, a key role is played by the combination of incidence angle, soil properties and surface roughness. An
335 example is presented by Chen et al. (2015a) as part of a review of archaeological marks in SAR imagery. A 1 m
336 resolution COSMO-SkyMed Spotlight HH polarization image acquired with 27.32° incidence angle revealed
337 shallow remains of walls and foundation close to the amphitheatre of Sabratha in Libya.

338 Figure 8 shows the clear archaeological mark detected over the deserted village of Dar es-Salaam, north of
339 the city of Homs in western Syria, using a 3 m resolution TerraSAR-X StripMap image. The size, shape and
340 location of the amplitude patterns match with the corresponding mark observed in Google Earth, thereby
341 proving that SAR imagery can be an effective alternative to optical data when the latter are not available or
342 cloud-covered. The radar backscatter also enhances the site as a distinctive feature compared with the nearly
343 regular orthogonal agricultural fields in the surroundings, also testifying the extensive program of cadastration
344 or centuriation of the basalt landscape. Dar es-Salaam is nowadays mostly a mass of rubble, with no standing
345 structures. These apparently were demolished over the centuries to source good worked stone for use in the

346 local farms. Therefore the spatial investigation of the site extent is crucial to understand the relationship
347 between Dar es-Salaam and the field systems, alongside its physical outreach, i.e. the area of influence and
348 control on the surrounding hinterland.

349



350

351 **Figure 8:** Detection of the archaeological features of the deserted village of Dar es-Salaam, north-west of
352 Homs, Syria. (a) Google Earth image (© DigitalGlobe 2015), (b) TerraSAR-X 3-m resolution StripMap VV
353 image (© DLR 2016) from which the site and surrounding agricultural fields are clearly visible.

354

355 **4.2 Condition assessment and environmental monitoring**

356 There is a wealth of recent literature concerning the use of multi-temporal InSAR for condition assessment of
357 monuments and sites threatened by natural and human-induced hazards (Cigna et al., 2012, 2014; Tapete and
358 Cigna, 2012a,b; Pratesi et al., 2015; Tapete et al., 2012, 2013a, 2015a; Zhou et al., 2015). Multi-temporal
359 InSAR provides sparse grids of point-wise deformation estimates that inform us about the stability of the objects
360 on the ground.

361 On the other side, amplitude change detection techniques (see section 3.2.1) highlight alteration of the landscape
362 and heritage assets in the form of backscatter change patterns (Figure 5b). At a regional scale this can be
363 exploited to investigate the impact of land surface dynamics occurring in a river catchment (Cigna et al., 2013)
364 or as a consequence of extensive cultivation. Geospatial analysis of backscatter changes can suggest a
365 correlation between the distribution and extension of seasonal floodable areas and human settlements (Conesa et
366 al., 2014). At local scale, depending on the spatial resolution of SAR imagery used, it is possible to identify
367 changes due to intentional alteration of archaeological features, such as illegal excavations (Tapete et al.,

368 2013b). In this regard, the new TerraSAR-X Staring Spotlight mode is opening a new frontier, as it brings, for
369 the first time, SAR data to image looting feature at resolutions comparable with VHR QuickBird, GeoEye and
370 WorldView optical imagery (Tapete et al., 2016).

371 As mentioned in section 3.2.2, interferometric coherence provides another option to investigate the
372 environmental impact on cultural landscape and features (e.g., Ruescas et al., 2009; Baade and Schullius,
373 2010) and is increasingly used in post-disaster damage assessment.

374 Last but not least, it is worth mentioning that the availability of SAR image stacks can be beneficial to analyse,
375 on a seasonal or yearly basis, geomorphological features relating to past, even vanished or hidden landscapes,
376 such as Quaternary paleo-environments and paleo-shorelines (Bachofer et al., 2014).

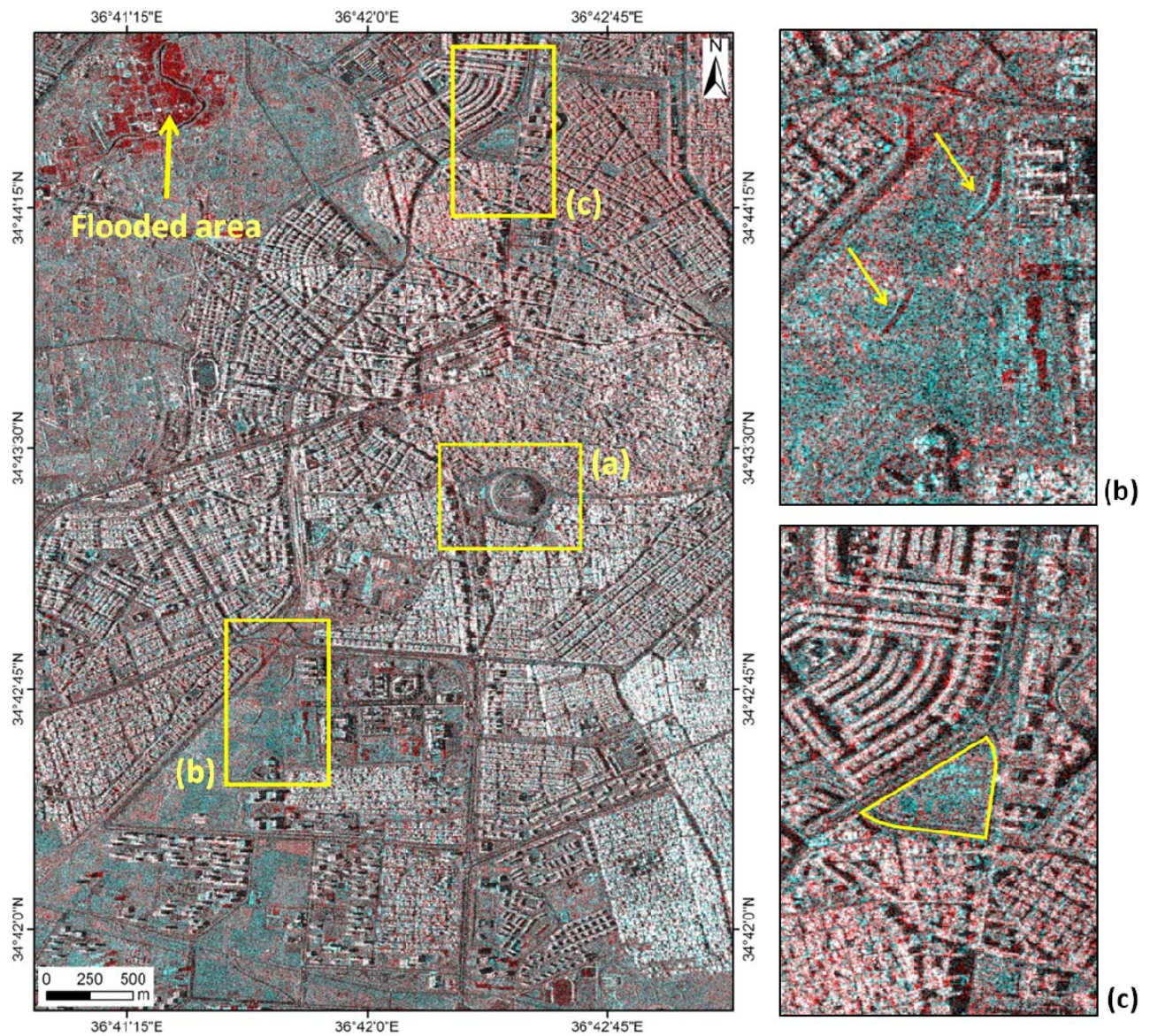
377 ***4.3 Damage assessment in areas of conflict***

378 An area where SAR can complement optical remote sensing is in the assessment of war damages to support the
379 monitoring and protection of cultural heritage in situation of crisis, such as those ongoing in the Middle East and
380 northern Africa. The advantage of operating under any weather conditions and the possibility of acquiring on a
381 regular basis make SAR a gap-filler and an alternative option to using optical or aerial imagery whenever the
382 latter are not feasible.

383 Figure 9 shows the results of change detection analysis in the city of Homs based on the comparison of 3 m
384 resolution TerraSAR-X and TanDEM-X VV polarization StripMap acquisitions of August 2009 and December
385 2014, i.e. prior to and after major impacts of the recent Syrian civil war. Damages and war-related alteration
386 include (a) military blockages and (b) excavations and trenches (Tapete et al., 2015c). Background information
387 and environmental considerations also help to correctly interpret the other change patterns, apparently not due to
388 the conflict such as pre-war demolitions (c) and the flooded area in the top left corner of Figure 9.

389 As mentioned in section 2.1.2, this is a type of analysis that might be undertaken in emergency contexts using
390 Sentinel-1 StripMap mode over wide areas of investigation, coupled with local-scale assessment based on
391 exploitation of L- and X-band high to very high resolution imagery.

392



393

394 **Figure 9:** RC colour composite of 17 August 2009 and 05 December 2014 VV SM TSX over Homs, Syria (©
 395 DLR 2016), with examples of damages and changes in the urban setting: (a) Homs Tell with evidence of
 396 alteration at the bottom of the tell; (b) trenches and embankments in the area of Homs University; (c) Area of
 397 pre-war building demolition, northern quarter of Homs (modified from Tapete et al., 2015c).

398

399 5 CONCLUSIONS

400 Clear evidence that proves that SAR is now recognised as a valuable technology for investigating archaeology is
 401 the increased number of books and dedicated special issues which have been published on this subject in recent
 402 years (e.g. Wiseman and El-Baz, 2007; Lasaponara and Masini, 2013). SAR-based heritage studies not only

403 involve image analysts, but also archaeologists in a joint effort to improve, if not even develop, SAR image
404 processing techniques to specifically address archaeological questions.

405 The increased accessibility to SAR data at different spatial resolution and temporal coverage certainly plays a
406 key role in encouraging scientists to undertake tests and pilot studies. But it is the different type of information
407 provided by SAR compared with other Earth Observation techniques – e.g. soil penetration, data to extract
408 topography, nearly regular acquisitions, and visibility in areas where optical sensors do not perform effectively
409 – which likely explains why this technology is increasingly being interrogated by archaeologists, mostly in
410 collaboration with remote sensing experts. The evidence found in the literature is that research outputs coming
411 out from such collaborative projects are increasing, thus suggesting that teamwork between different profiles
412 and professionals is helping to make SAR be more used in archaeology.

413 As demonstrated in this paper, the type of research currently undertaken with SAR can generate the following
414 scientific, cultural and social impacts:

- 415 • retrieval of proxies for surface morphological changes which can inform the decision-making process of
416 local authorities and stakeholders to implement measures to mitigate anthropogenic effects on the cultural
417 landscape;
- 418 • updated knowledge of subtle to monumental archaeological features proving earlier human occupation of
419 the landscape and representing the tangible signs of nations' cultural identity. This is particularly crucial in
420 developing countries and landscapes at risk of vanishing due to urbanisation or intentional destruction;
- 421 • compelling evidence to underpin quantitative assessment of the scale and rate of damage to archaeological
422 heritage and landscape, especially in accessible areas due to logistical constraints or security reasons.

423 Along these directions, SAR archaeological remote sensing can further develop, benefitting of increasing
424 consistent archives at increasing spatial resolution and temporal frequency. Development and testing of
425 algorithms for pattern recognition is undoubtedly another key area that would require more investigation,
426 although recent research such as Di Iorio et al. (2010) and Tapete et al. (2016) prove that great progress has
427 been already done in this regard.

428 Whilst opportunities to access SAR data from space are increasing, training on how to use these data and
429 demonstration of their potential value for archaeological study appear to be practical ways forward to fill the
430 gap between the specialist format of SAR data and the archaeology community, and support the transfer of SAR
431 technology into archaeological practice.

432 **ACKNOWLEDGEMENTS**

433 TerraSAR-X and TanDEM-X imagery of Syrian sites was provided by the German Aerospace Center (DLR) via
434 the TSX-New-Modes-2013 LAN2377 and TDX XTI-HYDR0399 grants. ENVISAT ASAR data over Apamea
435 (Syria) and the Nasca region (Peru) were provided by ESA via the Cat-1 projects id. 28439 and 11073,
436 respectively. Sentinel-1A data were accessed from ESA's Sentinels Scientific Data Hub. If not otherwise
437 specified, data processing was carried out using GAMMA SAR and Interferometry Software licensed to BGS,
438 NERC. The authors publish with the permission of the Executive Director of BGS, NERC.

439 **REFERENCES**

- 440 Adams R, Brown W, Culbert T (1981) Radar Mapping, Archeology, and Ancient Maya Land Use. *Science*
441 213:1457–1463
- 442 Agapiou, A., Lysandrou, V. (2015) Remote sensing archaeology: Tracking and mapping evolution in European
443 scientific literature from 1999 to 2015. *Journal of Archaeological Science: Reports* 4: 192-200.
- 444 Baade J, Schullius C (2010) High-resolution mapping of fluvial landform change in arid environments using
445 TerraSAR-X images. In: *Geoscience and Remote Sensing Symposium (IGARSS), 2010 IEEE International*, p
446 2159–2162
- 447 Bachofer F, Quénehervé G, Märker M (2014) The Delineation of Paleo-Shorelines in the Lake Manyara Basin
448 Using TerraSAR-X Data. *Remote Sens* 6:2195–2212.
- 449 Blom, RG, Crippen, RE, Zarins, J, Hedges, GR (2000) Remote sensing, Shuttle Radar Topographic Mapper
450 data, and ancient frankincense trade routes. In: *Geoscience and Remote Sensing Symposium, 2000.*
451 *Proceedings. IGARSS 2000. IEEE 2000 International*, Honolulu, HI, 2000, pp. 2477-2479 vol.6.
- 452 Chen F, Lasaponara R, Masini N (2015a) An overview of satellite synthetic aperture radar remote sensing in
453 archaeology: From site detection to monitoring. *J Cult Herit*.
- 454 Chen F, Masini N, Yang R et al (2015b) A Space View of Radar Archaeological Marks: First Applications of
455 COSMO-SkyMed X-Band Data. *Remote Sens* 7:24–50
- 456 Cigna F, Del Ventisette C, Gigli G et al (2012) Ground instability in the old town of Agrigento (Italy) depicted
457 by on-site investigations and Persistent Scatterers data. *Nat Hazards Earth Syst Sci* 12:3589–3603

- 458 Cigna F, Tapete D, Lasaponara R et al (2013) Amplitude change detection with Envisat ASAR to image the
459 cultural landscape of the Nasca region, Peru. *Archaeol Prospect* 20:117–131
- 460 Cigna F, Lasaponara R., Masini N et al (2014) Persistent Scatterer Interferometry Processing of COSMO-
461 SkyMed StripMap HIMAGE Time Series to Depict Deformation of the Historic Centre of Rome, Italy.
462 *Remote Sens* 6:12593–12618
- 463 Comer D, Blom R, Golden C, Quilter J, Chapman B (2005) Inventory of Archaeological Sites Using Radar and
464 Multispectral Data. Lecture presented at National Geographic Society, Washington, D.C.
- 465 Conesa F, Devanthery N, Balbo AL et al (2014) Use of satellite SAR for understanding long-term human
466 occupation dynamics in the monsoonal semi-arid plains of North Gujarat, India. *Remote Sensing*, 6 (11)
467 (2014), pp. 11420–11443.
- 468 Dore N, Patruno J, Pottier E et al (2013) New research in polarimetric SAR technique for archaeological
469 purposes using ALOS PALSAR data. *Archaeol Prospect* 20:79–87
- 470 Di Iorio, A., Straccia, N., Carlucci, R (2010) Advancement in automatic monitoring and detection of
471 archaeological sites using a hybrid process of Remote Sensing, GIS Techniques and a Shape Detection
472 Algorithm. *Remote Sensing for Science, Education, and Natural and Cultural Heritage. EARSeL*, 2010
473 Accessible at [http://www.earsel.org/symposia/2010-symposium-Paris/Proceedings/EARSeL-Symposium-](http://www.earsel.org/symposia/2010-symposium-Paris/Proceedings/EARSeL-Symposium-2010_2-01.pdf)
474 [2010_2-01.pdf](http://www.earsel.org/symposia/2010-symposium-Paris/Proceedings/EARSeL-Symposium-2010_2-01.pdf)
- 475 Elachi C, Roth L, Schaber G (1984) Spaceborne Radar Subsurface Imaging in Hyperarid Regions. *IEEE T*
476 *Geosci Remote* 4:383–387
- 477 El-Baz F (1998) Prehistoric artifacts near paleo-channels revealed by radar images in the western desert of
478 Egypt. In: *Remote Sensing in Archaeology from Spacecraft, Aircraft, on Land, and in the Deep Sea*, Boston
479 University, Boston
- 480 Erasmi S, Rosenbauer R, Buchbach R et al (2014) Evaluating the Quality and Accuracy of TanDEM-X Digital
481 Elevation Models at Archaeological Sites in the Cilician Plain, Turkey. *Remote Sens* 6:9475–9493
- 482 ESA (2007) TM-19 InSAR Principles: Guidelines for SAR Interferometry Processing and Interpretation. Part B
483 InSAR processing: a practical approach. TM-19_ptB http://www.esa.int/esapub/tm/tm19/TM-19_ptB.pdf
- 484 ESA (2013) ESA Sentinel-1 User Handbook. ESA Standard Document, GMES-S1OP-EOPG-TN-13-0001. 1
485 September 2013, 80 pp. <https://sentinel.esa.int/>

486 ESA (2015) SENTINEL-1 SAR Technical Guide. Glossary. Accessible at
487 <https://sentinel.esa.int/web/sentinel/sentinel-1-sar-wiki/-/wiki/Sentinel%20One/Glossary>

488 ESA-EARSeL (2015) 3rd ESA-EARSeL course on remote sensing for archaeology - Training, European Space
489 Agency. Accessible at <http://earth.esa.int/heritage/2015-events/15m38/training.html>

490 Evans, D, Pottier, C, Fletcher, R., Hensley, S., Tapley, I., Milne, A., Barbetti, M. (2007) A comprehensive
491 archaeological map of the world's largest preindustrial settlement complex at Angkor, Cambodia.
492 Proceedings of the National Academy of Sciences of the United States of America 104(36): 14277-14282.

493 Farr TG, Rosen PA, Caro E et al (2007) The Shuttle Radar Topography Mission. Rev Geophys 45,
494 RG2004/2007. doi:10.1029/2005RG000183

495 Gaber A, Koch M, Griesh MH et al (2013) Near-surface imaging of a buried foundation in the Western Desert,
496 Egypt, using space-borne and ground penetrating radar. J Archaeol Sci 40: 1946–1955

497 Gaber A, Soliman F, Koch M et al (2015) Using full-polarimetric SAR data to characterize the surface
498 sediments in desert areas: A case study in El-Gallaba Plain, Egypt. Remote Sens Environ 16:11–28

499 Guo, Huadong; Li, XinWu; Liu, Guang; Zhang, Lu; Zhu, LanWei; Yang, Huaining; Yan, Shiyong; Ruan,
500 Zhixin (2011) Study For Land SurfaCe Properties With Alos Palsar. Accessible at
501 <https://repository.exst.jaxa.jp/dspace/bitstream/a-is/16537/1/65135024.pdf>

502 Lasaponara R, Masini N (2013) Satellite synthetic aperture radar in archaeology and cultural landscape: An
503 overview. Archaeol Prospect 20:71–78

504 Lira, J, Lopez, P., Rodriguez, A. (2005) Detection of Maya's archaeological sites using high resolution radar
505 images. International Journal of Remote Sensing 26(6): 1245-1260.

506 Kurtcebe, F, Pfeifer, N, Ipbuker, C (2010) Remotely sensed archeology: Recent applications with
507 DAICHI (Conference Paper). In: 31st Asian Conference on Remote Sensing 2010, ACRS 2010; Hanoi; Viet
508 Nam; Volume 2, 2010, pp. 1168-1175.

509 Menze, BH, Ur, JA, Sherratt, AG (2006) Detection of Ancient Settlement Mounds: Archaeological Survey
510 Based on the SRTM Terrain Model. Photogrammetric Engineering & Remote Sensing 72(3): 321–327.

511 Mittermayer J, Wollstadt S, Prats-Iraola P et al (2014). The TerraSAR-X Staring Spotlight Mode Concept. IEEE
512 T Geosci Remote 52:3695–3706

513 Moore E, Freeman T, Hensley S (2007) Spaceborne and Airborne Radar at Angkor: Introducing New
514 technology to the Ancient Site. In: J.R.Wiseman & F. El-Baz (eds) Remote Sensing in Archaeology,

515 technology to the Ancient Site. In: J.R.Wiseman & F. El-Baz (eds) Remote Sensing in Archaeology,
516 Springer, pp. 185-218.

517 Patruno J, Dore N, Crespi M et al (2013) Polarimetric multifrequency and multi-incidence SAR sensors analysis
518 for archaeological purposes. *Archaeol Prospect* 20:89–96

519 Pratesi F, Tapete D, Terenzi G et al (2015) Rating health and stability of engineering structures via classification
520 indexes of InSAR Persistent Scatterers *Int J Appl Earth Obs* 40:81–90

521 Ruescas AB, Delgado JM, Costantini F et al (2009) Change detection by interferometric coherence in Nasca
522 Lines, Peru (1997–2004). In: *Fringe Workshop Proceedings 2009*, European Space Agency SP-677, ESA-
523 ESRIN, Frascati, 30 November– 4 December 2009

524 Stewart C, Lasaponara R, Schiavon G (2014) Multi-frequency, polarimetric SAR analysis for archaeological
525 prospection. *Int J Appl Earth Obs* 28:211–219

526 Tapete D, Cigna F (2012a) Rapid mapping and deformation analysis over cultural heritage and rural sites based
527 on Persistent Scatterer Interferometry. *Int J Geophys*. doi:10.1155/2012/618609

528 Tapete D, Cigna F (2012b) Site-specific analysis of deformation patterns on archaeological heritage by satellite
529 radar interferometry. In: *20th International Materials Research Congress, Symposium 8 Cultural Heritage and*
530 *Archaeological Issues in Materials Science*, MRS Proceedings 1374, Cambridge University Press, p 283–295

531 Tapete, D., Cigna, F. (2015) Change detection in cultural landscapes. In: *3rd ESA-EARSeL course on remote*
532 *sensing for archaeology - Training*, European Space Agency. Accessible at [http://earth.esa.int/heritage/2015-](http://earth.esa.int/heritage/2015-events/15m38/Training/14_Tapete_Cigna.pdf)
533 [events/15m38/Training/14_Tapete_Cigna.pdf](http://earth.esa.int/heritage/2015-events/15m38/Training/14_Tapete_Cigna.pdf)

534 Tapete D, Cigna F, Donoghue D.N.M. (2016) ‘Looting marks’ in space-borne SAR imagery: Measuring rates of
535 archaeological looting in Apamea (Syria) with TerraSAR-X Staring Spotlight. *Remote Sensing of*
536 *Environment* 178: 42-58.

537 Tapete D, Fanti R, Cecchi R et al (2012) Satellite radar interferometry for monitoring and early-stage warning
538 of structural instability in archaeological sites. *J Geophys Eng* 9:S10–S25

539 Tapete D, Casagli N, Luzi G et al (2013a) Integrating radar and laser-based remote sensing techniques for
540 monitoring structural deformation of archaeological monuments. *J Archaeol Sci* 40:176–189

541 Tapete D, Cigna F, Masini N et al (2013b) Prospection and Monitoring of the Archaeological Heritage of
542 Nasca, Peru, with ENVISAT ASAR. *Archaeol Prospect* 20:133–147

543 Tapete D, Morelli S, Fanti R et al (2015a) Localising deformation along the elevation of linear structures: An
544 experiment with space-borne InSAR and RTK GPS on the Roman Aqueducts in Rome, Italy. *Appl Geogr*
545 58:65–83

546 Tapete D, Cigna F, Lasaponara R et al (2015b) Multi-scale detection of changing cultural landscapes in Nasca
547 (Peru) through ENVISAT ASAR and TerraSAR-X. In: Lollino G et al (eds), *Engineering Geology for*
548 *Society and Territory - Volume 8*, Springer International Publishing, p 339–343

549 Tapete D, Cigna F, Donoghue DNM et al (2015c) Mapping changes and damages in areas of conflict: from
550 archive C-band data to new HR X-band imagery, towards the Sentinels. In: *Proceedings of FRINGE'15:*
551 *Advances in the Science and Applications of SAR Interferometry and Sentinel-1 InSAR Workshop*, Frascati,
552 Italy, 23-27 March 2015, Ouwehand L., Ed., ESA Publication SP-731. doi:10.5270/Fringe2015.149

553 Wiseman J, El-Baz F (eds) (2007) *Remote Sensing in Archaeology*. Springer, New York

554 Zhou W, Chen F, Guo H (2015) Differential radar interferometry for structural and ground deformation
555 monitoring: a new tool for the conservation and sustainability of cultural heritage sites. *Sustainability*
556 7:1712–1729